



HAL
open science

Global Marine Heatwaves Under Different Flavors of ENSO

Catherine H. Gregory, Camila Artana, Skylar Lama, Dalena León-Fonfay, Jacopo Sala, Fuan Xiao, Tongtong Xu, Antonietta Capotondi, Cristian Martinez-Villalobos, Neil J. Holbrook

► **To cite this version:**

Catherine H. Gregory, Camila Artana, Skylar Lama, Dalena León-Fonfay, Jacopo Sala, et al.. Global Marine Heatwaves Under Different Flavors of ENSO. *Geophysical Research Letters*, 2024, 51, 10.1029/2024GL110399 . insu-04821266

HAL Id: insu-04821266

<https://insu.hal.science/insu-04821266v1>

Submitted on 5 Dec 2024

HAL is a multi-disciplinary open access archive for the deposit and dissemination of scientific research documents, whether they are published or not. The documents may come from teaching and research institutions in France or abroad, or from public or private research centers.

L'archive ouverte pluridisciplinaire **HAL**, est destinée au dépôt et à la diffusion de documents scientifiques de niveau recherche, publiés ou non, émanant des établissements d'enseignement et de recherche français ou étrangers, des laboratoires publics ou privés.



Distributed under a Creative Commons Attribution 4.0 International License

Geophysical Research Letters®

RESEARCH LETTER

10.1029/2024GL110399

Global Marine Heatwaves Under Different Flavors of ENSO



Key Points:

- Robust links between global marine heatwaves and El Niño–Southern Oscillation (ENSO) diversity are established using 10,000 years of samples from a linear inverse model
- Marine heatwave (MHW) intensity and frequency in the Northeast Pacific increase significantly during Central Pacific El Niño events
- MHW intensity and frequency are significantly enhanced in Western Australia during Central Pacific La Niña events

Supporting Information:

Supporting Information may be found in the online version of this article.

Correspondence to:

C. H. Gregory,
Catherine.Gregory@utas.edu.au








Citation:

Gregory, C. H., Artana, C., Lama, S., León-FonFay, D., Sala, J., Xiao, F., et al. (2024). Global marine heatwaves under different flavors of ENSO. *Geophysical Research Letters*, 51, e2024GL110399. <https://doi.org/10.1029/2024GL110399>

Received 9 JUN 2024
Accepted 27 AUG 2024

Author Contributions:

Conceptualization: Catherine H. Gregory, Camila Artana, Antonietta Capotondi, Cristian Martinez-Villalobos, Neil J. Holbrook
Methodology: Catherine H. Gregory, Camila Artana, Skylar Lama, Dalena León-FonFay
Visualization: Catherine H. Gregory, Camila Artana, Skylar Lama, Dalena León-FonFay
Writing – original draft: Catherine H. Gregory, Camila Artana, Skylar Lama, Dalena León-FonFay, Jacopo Sala, Fuan Xiao

Catherine H. Gregory^{1,2} , Camila Artana³ , Skylar Lama^{4,5}, Dalena León-FonFay⁶, Jacopo Sala⁷ , Fuan Xiao⁸ , Tongtong Xu^{9,10} , Antonietta Capotondi^{9,10} , Cristian Martinez-Villalobos^{11,12} , and Neil J. Holbrook^{1,2} 

¹Institute for Marine and Antarctic Studies, University of Tasmania, Hobart, TAS, Australia, ²Australian Research Council Centre of Excellence for Climate Extremes, University of Tasmania, Hobart, TAS, Australia, ³LOCEAN-IPSL, Sorbonne Université (UPMC), Paris, France, ⁴School of Earth and Atmospheric Science, Georgia Institute of Technology, Atlanta, GA, USA, ⁵Program in Ocean Science and Engineering, Georgia Institute of Technology, Atlanta, GA, USA, ⁶Institute of Coastal Systems, Helmholtz-Zentrum Hereon, Geesthacht, Germany, ⁷Department of Atmospheric and Oceanic Sciences, University of Colorado Boulder, Boulder, CO, USA, ⁸School of Geography and Remote Sensing, Guangzhou University, Guangzhou, China, ⁹Cooperative Institute for Research in Environmental Sciences, University of Colorado, Boulder, CO, USA, ¹⁰Physical Sciences Laboratory, NOAA, Boulder, CO, USA, ¹¹Faculty of Engineering and Science, Universidad Adolfo Ibáñez, Santiago, Chile, ¹²Data Observatory Foundation, ANID Technology Center No. DO210001, Santiago, Chile

Abstract Marine heatwaves (MHWs) have caused devastating ecological and socioeconomic impacts worldwide. Understanding the connection of regional events to large-scale climatic drivers is key for enhancing predictability and mitigating MHW impacts. Despite the reported connection between MHWs globally and El Niño–Southern Oscillation (ENSO), establishing statistically significant links between different types of ENSO events and MHWs remains challenging due to the limited duration of observational data. Here, we use 10,000 years of simulations from a Linear Inverse Model (LIM) to address this issue. Our findings reveal distinct connections between MHWs and ENSO, with diverging influences from different flavors of El Niño and La Niña events. In addition, under long-lasting El Niño conditions, the likelihood of MHWs increases by up to 12-fold in the Indian and Pacific Oceans. This study highlights the global connections between ENSO diversity and variations in MHW events.

Plain Language Summary Marine heatwaves (MHWs) are periods of prolonged, extremely warm ocean temperatures that have caused widespread ecological and socioeconomic impacts worldwide. The predictability of these events can be improved if we can find connections between regional events and larger climatic drivers, such as El Niño–Southern Oscillation (ENSO). Both the positive phase of ENSO, El Niño, and its negative phase, La Niña, have been linked to MHWs in various parts of the world. However, not all El Niño and La Niña events are the same, leading to uncertainty in the relationship between ENSO and MHWs. Due to the limited duration of the observational record, a major issue arises with the lack of examples of different types of El Niño and La Niña events in observations. To overcome this challenge, we utilized 10,000 years of simulated data from a near-global linear inverse model to generate many more samples of possible global ocean temperature configurations. We find strong differences between regional MHWs and different types of El Niño and La Niña events. In some regions, the probability of MHWs is 12 times more likely under long-lasting El Niño events.

1. Introduction

Marine heatwaves (MHWs) are characterized by prolonged periods of anomalously warm ocean temperatures at a given location (Hobday et al., 2016). In recent decades these extreme events have been the focus of many studies due to their impacts on marine biodiversity and ecosystem services (Smale et al., 2019), as well as biological (Smith et al., 2023) and socioeconomic systems (Smith et al., 2021). Gaining a comprehensive understanding of the drivers influencing the occurrence of these thermal extremes is essential for assessing their predictability and improving forecasting skill, which can aid marine resource managers in the development of proactive management strategies (Holbrook et al., 2019, 2020).

El Niño–Southern Oscillation (ENSO) is the leading driver of seasonal-to-interannual climate variability globally (Lenssen et al., 2020; Neelin et al., 1998; Wallace et al., 1998), exerting substantial influence on climate patterns and atmospheric circulation well beyond the tropical Pacific. There are several regions where MHWs have well known connections with ENSO. The Western Australian region, for example, is strongly influenced by the

© 2024. The Author(s).

This is an open access article under the terms of the [Creative Commons Attribution License](https://creativecommons.org/licenses/by/4.0/), which permits use, distribution and reproduction in any medium, provided the original work is properly cited.

Writing – review & editing: Catherine H. Gregory, Camila Artana, Skylar Lama, Dalena León-FonFay, Jacopo Sala, Fuan Xiao, Tongtong Xu, Antonietta Capotondi, Cristian Martinez-Villalobos, Neil J. Holbrook

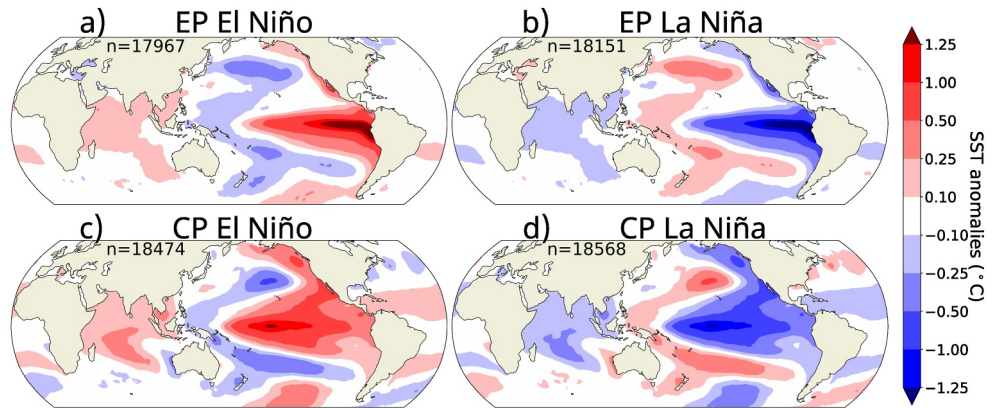


Figure 1. Average SST anomalies during (a) EP El Niño, (b) EP La Niña, (c) CP El Niño, and (d) CP La Niña computed as composite maps from the LIM simulations. The n -value represents the number of months in each of the composite maps.

poleward flowing warm water current known as the Leeuwin Current (Cresswell & Golding, 1980) which is strengthened during La Niña periods due to the enhancement of the easterly trade winds in the western equatorial Pacific, resulting in increased transport of upper-ocean warm waters from the western Pacific to the eastern Indian Ocean, via the Indonesian archipelago (Meyers, 1996). Associated with the very strong 2010/11 La Niña event, the Western Australia region experienced MHWs that were unprecedented for that time, lasting for more than 10 weeks and reaching around 5°C above normal (Pearce & Feng, 2013).

The Northeast Pacific is another region influenced by ENSO. Two notable MHWs, one during 2013–2015 (Bond et al., 2015; Di Lorenzo & Mantua, 2016) and the other during 2019 (Amaya et al., 2020), generated large-scale “warm blobs” in the Northeast Pacific that led to devastating impacts across the region, including prolonged consequences for marine ecosystems along the US West Coast (Cheung & Frölicher, 2020; Wyatt et al., 2022). While the onset of the 2013–2015 MHW was attributed to a resilient atmospheric ridge, which weakened the climatological Aleutian Low and reduced surface winds, the event's evolution and prolonged duration was linked to large-scale Pacific climate variability, particularly ENSO, via atmospheric teleconnections (Capotondi et al., 2022; Ren et al., 2023; Xu et al., 2021). The 2019 event was also linked to the weakening of the North Pacific High, which was partly driven by the conditions of the tropical Pacific Ocean (Amaya et al., 2020). Holbrook et al. (2019) also highlighted this connection by showing that the number of MHW days in the northeast Pacific nearly doubles during El Niño periods and nearly halves during La Niña periods.

ENSO comprises different flavors, distinguished by the spatial distribution of sea surface temperature (SST) anomalies (Capotondi et al., 2015; Timmermann et al., 2018), which were associated to different impacts (e.g., Ashok et al., 2007) (Figure 1). Thus, the ENSO-MHW connection can be expected to also be affected by the diversity of ENSO events. The canonical eastern Pacific (EP) El Niño is characterized by warm SST anomalies in the central and eastern equatorial Pacific (Figure 1a), whereas the central Pacific (CP) El Niño is characterized by warm SST anomalies in the central Pacific, but with little or no warming in the eastern Pacific (Kao & Yu, 2009; Newman et al., 2011) (Figure 1c). In contrast, during La Niña, warm anomalies are observed in the western equatorial Pacific, with cold anomalies concentrated in the central region during CP La Niñas (Figure 1d) or in the eastern Pacific during EP La Niñas (Figure 1b). There are also mixed ENSO patterns, which exhibit characteristics of both EP and CP El Niño/La Niña types (Gen et al., 2010).

Previous studies (e.g., Capotondi et al., 2019; Capotondi et al., 2022), have shown a strong association of Northeast Pacific MHWs with SST anomalies in the central equatorial Pacific typical of CP El Niño events. The most intense MHW in Western Australia occurred in conjunction with the CP La Niña of 2011–2012 (Feng et al., 2013), also suggesting a sensitivity of Western Australia MHWs to the location of La Niña SST anomalies. However, understanding the influence of these different types of ENSOs on MHWs is complicated by the relatively limited number of these events in the observational record, preventing the establishment of robust statistical connections. Previous studies have helped to overcome this shortcoming using synthetic data from linear inverse models (LIMs) (Penland & Magorian, 1993; Penland & Sardeshmukh, 1995). A LIM provides a linear approximation to the underlying dynamics using observed data while characterizing the nonlinear and fast-

decorrelating dynamics as stochastic forcings. This empirical model can be integrated forward in time to generate extensive sets of simulated data, with statistical properties similar to those of the training observational data. The value of these synthetic time series has been demonstrated in several previous studies (Capotondi & Sardeshmukh, 2017; Wang et al., 2023; Xu et al., 2022).

In this study, we utilize 120,000 months (10,000 years) of LIM simulation to explore global MHW statistics during CP and EP El Niño and La Niña periods. We also investigate the differences in long- and short-lived ENSO events and examine five key case study regions to assess specific teleconnections and impacts. By leveraging this information, tailored strategies to mitigate risks and optimize resource utilization in anticipation of MHWs may be developed.

2. Data and Methods

2.1. LIM Data

Long LIM simulations of SSTs from Xu et al. (2022) were used in this study (Xu, 2024). These LIM simulations were generated based on averaged SST products spanning 60 years (1958–2017) from Hadley Center Sea Ice and Sea Surface Temperature (HadISST) (Rayner et al., 2003), Extended Reconstructed Sea Surface Temperature version 5 (ERSSTv5) (Huang et al., 2015), and Centennial in situ Observation-Based Estimates (COBE) (Ishii et al., 2005). These simulations, with a horizontal resolution of $1^\circ \times 1^\circ$, span a record length of 120,000 months (10,000 years) and exhibit statistical behaviors akin to observed SSTs (see Xu et al. (2022) for more information), indicating the adequacy of the LIM-simulated data for our study. We have additionally tested the LIM's representation of ENSO diversity against the HadISST product showing that the LIM simulates well the spatial pattern of the two leading EOFs used to derive the CP and EP indices (Figure S3 in Supporting Information S1), the patterns of the different ENSO flavors (compare Figure 1 with Figure S4 in Supporting Information S1) and the distribution of ENSO indices (Figure S5 in Supporting Information S1). This is not surprising, as the LIM has been extensively used for studies of ENSO diversity (e.g., Capotondi & Sardeshmukh, 2015; Newman et al., 2011; Vimont et al., 2014).

2.2. ENSO Indices

Eastern Pacific (EP) and Central Pacific (CP) ENSO indices were derived using the methodology of Takahashi et al. (2011). An empirical orthogonal function analysis was conducted on the LIM SST anomalies in the equatorial Pacific region (10°S – 10°N) (Figure S2 in Supporting Information S1) and the first and second principal components (PC1 and PC2) were normalized and smoothed with a 1-2-1 filter to calculate the indices as follows:

$$\text{EP index} = (\text{PC1} - \text{PC2})/\sqrt{2}$$

$$\text{CP index} = (\text{PC1} + \text{PC2})/\sqrt{2}$$

When the index was sustained at values $>+1$ (<-1) $^\circ\text{C}$ for 5 months or greater, we considered this an El Niño (La Niña) event, with all other periods deemed to be neutral. We also separated these events into groups depending on their duration, with events lasting from 5 to 12 months classified as short-lived events and those lasting more than one year classified as long-lasting events. The frequency distribution of the CP and EP El Niño and La Niña event durations can be found in Figure S1 of Supporting Information S1.

2.3. MHW Metrics

As monthly data were analyzed, we considered any month with SST anomalies above the 95th percentile to be in a MHW state, following the previous studies of Jacox et al. (2020) and Capotondi et al. (2022). MHWs were computed for both long- and short-lasting EP and CP El Niño and La Niña events. The average intensity for MHW events during each of the categories was computed as the difference between the average SST anomaly of the events occurring during ENSO conditions and the average SST anomaly of events occurring during neutral months. This allowed us to compute the increased intensity connected to the relevant ENSO flavor and category.

We also considered the change in likelihood of a MHW occurrence during CP and EP El Niño and La Niña phases by comparing the likelihood (proportion) of events during an ENSO phase with the likelihood of events during neutral phases as in the equation:

$$\begin{aligned} &\text{Change in likelihood of MHW occurrence} \\ &= \frac{\text{Likelihood of events during ENSO phase} - \text{Likelihood of events during Neutral}}{\text{Likelihood of events during Neutral}} \times 100 \end{aligned}$$

Only those results significant at $\geq 95\%$ level using a student *t*-test (Student, 1908) were displayed. We accounted for serial correlations of the SST anomalies by using the lag-1 autocorrelation (ρ) to find an effective sample size ($n_{\text{eff}} = n \frac{1-\rho}{1+\rho}$), as in Marshall et al. (2014).

3. Results

Here, we first present the global spatial patterns of MHW intensity and likelihood of occurrence during short (5–12 months) and long (+13 months) lasting EP and CP El Niño and La Niña events. Then, we describe the local responses in several key regions of interest.

3.1. MHW Intensities

Here, we examine the changes in MHW intensity during El Niño and La Niña phases (including short- and long-lasting events) relative to MHWs occurring during neutral years (Figure 2). In general, we found that El Niño (Figure 2 upper box) periods were associated with higher MHW intensities over a wider spatial domain compared to La Niña periods (Figure 2 lower box). During El Niño periods, the strongest increases in MHW intensities were unsurprisingly found in the Pacific Ocean, with values $> +0.5^\circ\text{C}$. Strong signals were also found in the Indian and Atlantic Oceans, where increases in the range $0.03^\circ\text{C} - 0.15^\circ\text{C}$ (Figures 2a, 2b, 2e and 2f) are observed. During La Niña phases, MHW intensities up to $+0.3^\circ\text{C}$ above neutral states were found primarily in the western Pacific and were more extensive for longer event durations (Figures 2g and 2h).

Notable differences are also evident between average MHW intensities during CP versus EP ENSO types in the Pacific, Indian, and Atlantic Oceans. During CP El Niño events (Figures 2a and 2e), MHWs have increased intensities of up to 0.15°C , along US and Canadian coastlines, extending into open ocean, with larger intensity increase for longer events. This pattern becomes more confined to the coastlines during EP El Niño events (Figures 2b and 2f). In the Indian Ocean, large intensity changes are observed during both CP El Niño (Figures 2a and 2e) and EP El Niño events (Figures 2b and 2f). However, these anomalies extend to the Western Australian coast during EP El Niño periods, while neutral/cold anomalies are seen along Western Australia during CP events. In the tropical Atlantic, there are two pronounced bands of higher MHW intensity in the North and South Atlantic during CP El Niño (Figures 2a and 2e) while only the band in the South Atlantic is seen during EP El Niño (Figures 2b and 2f). During CP La Niña (Figures 2c and 2g), these bands of intensified MHWs are shifted further poleward, while a decrease in MHW intensity is seen at lower latitudes. Moreover, it was found that CP La Niña events are associated with increased MHW intensity along the west coast of Australia (mean intensity increase of 0.15°C), an increase that is not observed during EP La Niña events, while a reduction in MHW mean intensity of 0.1°C is seen in the northeast Pacific (Figures 2c and 2g).

There are also interesting differences in MHW characteristics when considering long-lasting (Figures 2e–2h) and short-lasting (Figures 2a–2d) ENSO events. Overall, we observed a reinforcement of the spatial patterns obtained with short-lasting ENSO events when considering long-lasting ENSO events, particularly in the Pacific and Indian Oceans. The intensity difference between shorter and longer-lasting CP El Niño events (Figure 2i) shows a pattern in the Pacific reminiscent of a decadal mode of variability described by Capotondi et al. (2022), connecting Northeast Pacific and central equatorial Pacific SST anomalies. The relatively large increase in Pacific MHW intensity during long-lasting CP events is consistent with the decadal component of CP ENSO variability (Capotondi et al., 2020; Sullivan et al., 2016). Long-lasting El Niño events (Figures 2e and 2f) are associated with MHWs with intensities of $+0.1^\circ\text{C}$ in the southwest Atlantic Ocean, while long-lasting EP La Niña (Figure 2h) periods show MHWs with intensities of $+0.1^\circ\text{C}$ in the Mediterranean and North Atlantic. While the Hawaiian Islands are not significantly impacted by MHWs during shorter lived EP La Niña periods (Figure 2d), during long-lasting EP La Niña events (Figure 2h), the meridional extent of MHWs increases in the North Pacific Ocean,

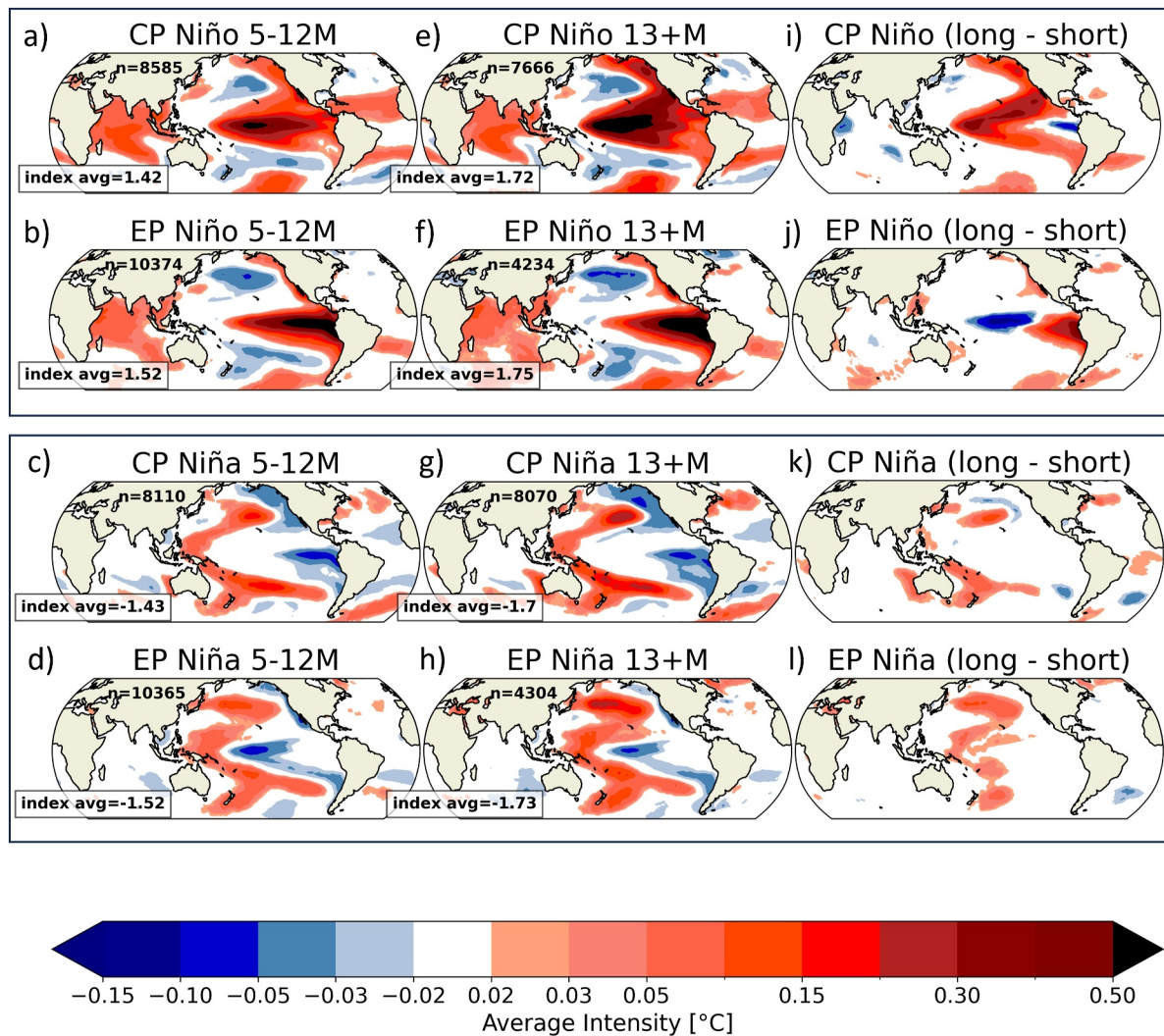


Figure 2. Changes in MHW intensity (compared to neutral states) based on the different flavors of El Niño (top box) and La Niña (bottom box), CP and EP, at varying durations, 5–12 months (a–d), and 13+ months (e–h), with the right column (i–l) showing the difference between long- and short-lasting events. Both red and blue color shadings represent statistically significant values at $\geq 95\%$ confidence level.

such that the Hawaiian Islands are impacted by MHWs with intensity differences of $\sim 0.2^\circ\text{C}$. Similarly, CP El Niños can affect the Hawaiian Islands due to the broader meridional scale of the tropical anomalies.

The patterns obtained with the LIM are generally consistent with those detected in observations (Figure S6 in Supporting Information S1), although the differences in MHW statistics obtained using observational data exhibit a larger amplitude, likely due to the smaller sample sizes for each type of event. However, while the patterns seen in the LIM data are statistically significant at $\geq 95\%$ confidence level for the entire globe, the differences seen in observations are statistically significant only in specific regions for specific event types. This is the case, for instance, in the Indian Ocean during CP, and especially EP, El Niño periods (Figure 2 upper box and Figure S6 in Supporting Information S1).

3.2. MHW Likelihood

ENSO also plays a significant role in the likelihood of MHWs in various regions around the world, either locally in the tropical Pacific, or remotely through atmospheric teleconnections (Holbrook et al., 2019; Sen Gupta et al., 2020). Here, we examine the changes in MHW likelihood during El Niño and La Niña phases relative to MHWs occurring during neutral years (Figure 3). During El Niño periods (Figures 3a–3d), we found an increase in the likelihood of MHWs of up to 12 times in the central/eastern Pacific Oceans, depending on the CP

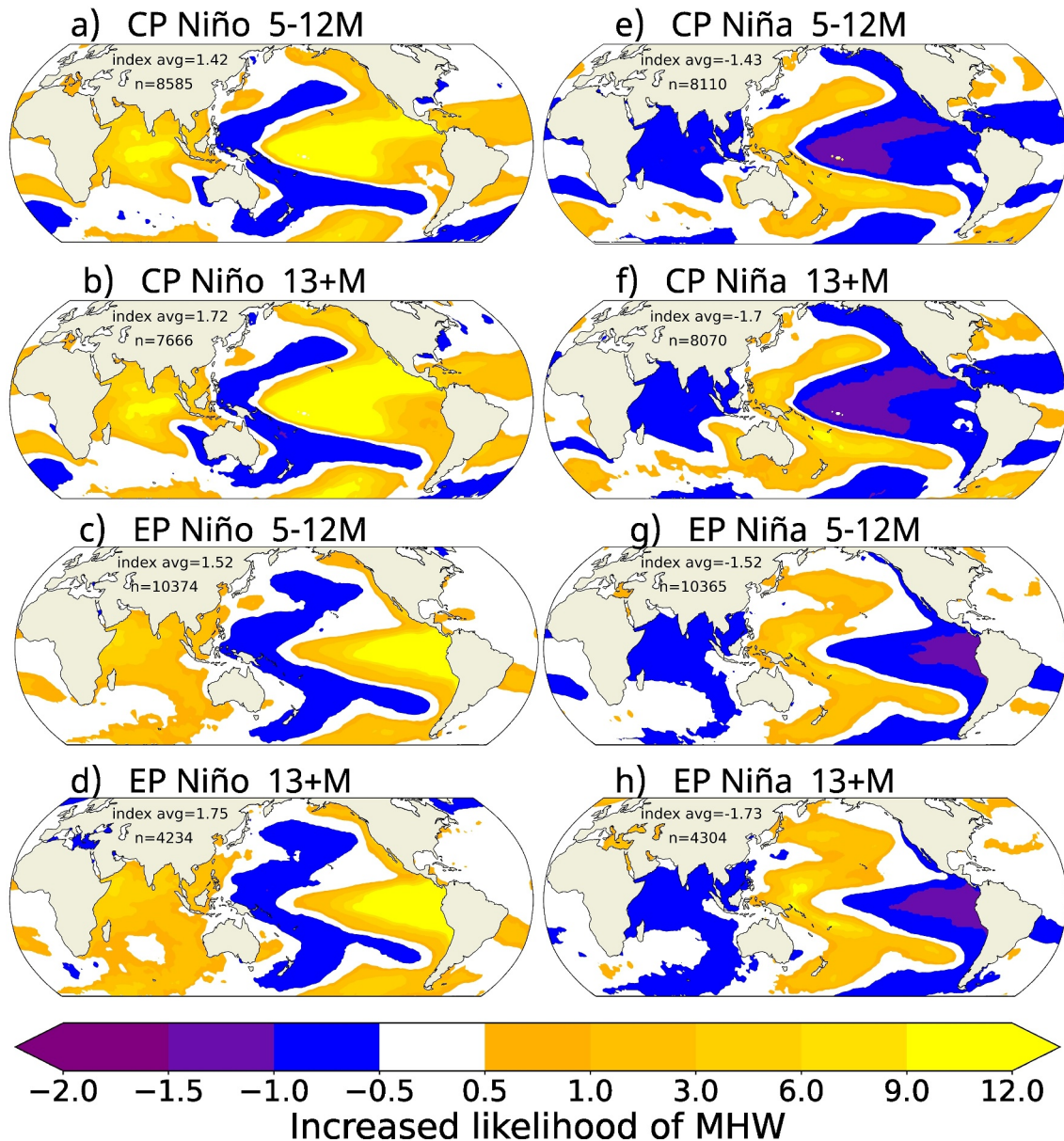


Figure 3. Changes in likelihoods (compared to neutral) of MHW occurrences during CP El Niño events of shorter durations (a) and longer durations (b), EP El Niño events of shorter durations (c) and longer durations (d), CP La Niña events of shorter durations (e) and longer durations (f) and EP La Niña events of shorter durations (g) and longer durations (h). Shadings represent statistically significant values at $\geq 95\%$ confidence level.

(Figures 3a and 3b) or EP (Figures 3c and 3d) flavor. Off the Pacific North and South American coasts, MHWs were found to be 1 to 6 times more frequent during both flavors of El Niño (Figures 3a–3d), in agreement with Carrasco et al. (2023). In the Indian Ocean, there is also a significant increase in MHW likelihood, with the ratio amplified by a factor of 9–12 in the central Indian Ocean during CP El Niño (Figures 3a and 3b). During EP Niño events (Figures 3c and 3d) the area of the Indian Ocean that has an increased likelihood of MHWs is larger, with an increase over the East African coast up to a factor of 6. Thus, not only do MHWs become more intense during El Niño periods in some regions, but they also become significantly more frequent.

During La Niña events (Figures 3e–3h), changes to MHW likelihoods lower compared to El Niño periods. Here, likelihoods of MHWs in the western Pacific Ocean increase on average by 3–6 times, with smaller regions, such as the Western Australian coastline, showing increased likelihood of up to 9 times during CP La Niña events (Figures 3e and 3f), slightly nearer to shore. MHWs in this region are strongly dependent on the type of La Niña

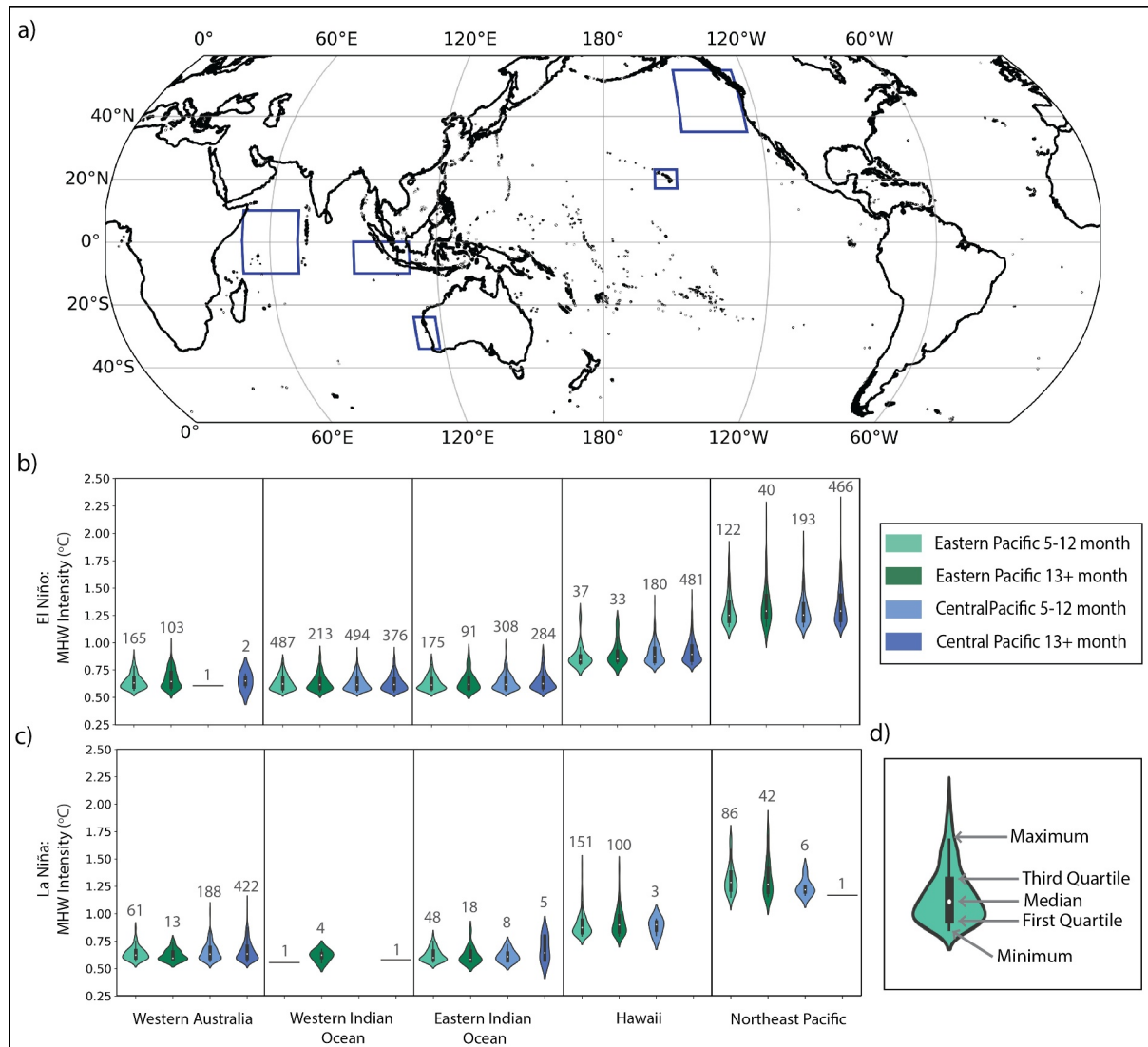


Figure 4. Global map with boxes around the five regions analyzed (a), and regionally averaged MHW intensity distributions during El Niño (b) and La Niña (c) phases based on the different flavors, CP and EP, at varying durations of 5–12 months and 13+ months. The numbers above each violin identify the sample sizes for the given event. The width of the violin indicates the frequency of a given value, while the inner box shows the quartiles of the distribution (d).

event, as an increase in MHW likelihood offshore of Western Australia does not occur during EP La Niña events (Figures 3g and 3h). As with the changes in intensity, we notice that the MHW likelihood increases in both magnitude and spatial extent over some regions with the increased duration of ENSO events.

3.3. Regional Analysis

From the global analysis above, we selected five key regions that showed distinct differences in MHW statistics either between El Niño and La Niña events, or between different El Niño or La Niña flavors. Figure 4a shows a global map with boxes indicating the five regions: Western Australia, strongly affected by MHWs during CP La Niña but not EP La Niña, the northeast Pacific, experiencing very high MHW intensity during both flavors of El Niño, the Hawaiian Islands, experiencing a high likelihood of MHW events during CP El Niño and EP La Niña, the western Indian Ocean, having little to no MHW during La Niña but a significant increase during both flavors of El Niño, and the eastern Indian Ocean, similarly experiencing a higher number of MHWs during El Niño, but also experiencing a number of events during EP La Niña periods. For these regions, we calculated area averaged

statistics to explore the regional relationships between MHW intensity and ENSO flavors. In Figures 4b and 4c, the violin plots show the distribution of the area averaged MHW intensities based on ENSO flavor and duration.

In the Western Australia region, the highest average intensity events occurred during long-lasting CP La Niña events (13+ months), with these phases also leading to the highest likelihood of MHWs (422 events) (Figure 4c). MHW events were least likely to occur in this region during CP El Niño phases (Figure 4b). However, EP El Niño events can be seen to positively contribute to MHW events (total 268 events). The mechanism for this influence does not appear to match that based on the Leeuwin Current extended flow, but it is rather associated with the eastward extension of the warm region in the western Indian Ocean, which is impacted by El Niño phases.

We also provide a quantitative comparison between the western and eastern Indian Ocean regions, with the violin plots showing an increase in likelihood of MHW events in both regions and for all flavors of El Niño (Figure 4b). In contrast, during La Niña periods, there is a notable absence of MHWs in the western Indian Ocean, while there are 66 events in the eastern Indian Ocean during EP La Niña events (Figure 4c).

MHWs in the Hawaiian box are more likely to occur during CP El Niño, with the long-lasting El Niño events tripling this likelihood, from 180 to 481 events (Figure 4b). Interestingly, the number of MHW events occurring during EP La Niña (151 events during short-lived EP La Niña and 101 during long-lived EP La Niña events) is greater than during EP El Niño events (37 during short-lived El Niño events and 33 during long-lived EP El Niño events), while almost no MHW events occurred around Hawaii during CP La Niña (Figure 4c). As previously noted, the broader meridional scale of the CP El Niño events allows the associated SST anomalies to affect Hawaii.

The northeast Pacific region has MHWs of the greatest intensities of our selected regions, with peak values of approximately +2.5°C (Figure 4b) during El Niño periods. These MHW events were more likely to occur during the longer lasting CP El Niño (consistent with Capotondi et al., 2022), with 466 events (Figure 4b). La Niña events appear to decrease the likelihood of MHW occurrences in this region, with a negligible number of events noted during CP La Niña (Figure 4c). The duration of ENSO itself affects the intensity of these events, with longer lasting events leading to MHWs of higher intensity, particularly during CP El Niño events.

4. Discussion and Conclusions

In this study, we have used linear inverse model (LIM)-simulated ENSO events, of different flavors and durations, to investigate their relationship with marine heatwaves (MHWs) across the globe. Previous studies have also considered the connection between MHWs and different ENSO flavors. In their 2019 study, Holbrook et al. showed that the percentage change of MHW days in the Western Australian region increased during both canonical La Niña periods, based on the Niño 3.4 index, and Modoki La Niña periods, a specific type of CP La Niña characterized by cooling in the central equatorial Pacific flanked by warming on either side (Ashok et al., 2007). Zhang et al. (2017) also found SSTs in Western Australia to be strongly correlated to Modoki La Niña. This supports our findings of an increase in the likelihood (Figures 3e and 3f) and intensities (Figures 2c and 2g) of MHWs in Western Australia during CP La Niña events. Similarly, Northeast Pacific MHWs show a stronger association with CP El Niño events, especially those events lasting more than 12 months, as previously suggested by Capotondi et al. (2019, 2022). However, while the limited duration of observational or reanalysis data sets used in previous studies prevented a robust assessment of the relationship between global MHWs and different ENSO types, our analysis allows the establishment of those relationships with high statistical significance.

Here we show statistics calculated using several thousand El Niño and La Niña events of both CP and EP types, and of different durations. This is made possible using data from a suite of LIM simulations (Xu et al., 2022) providing alternative realizations of the observational record, consistent with observed system dynamics and stochastic forcing. LIMs have proven useful in capturing changes in the state of ocean SSTs due to internal variability (Alexander et al., 2008; Capotondi et al., 2022; Capotondi & Sardeshmukh, 2017; Newman et al., 2016; Newman & Sardeshmukh, 2017) and statistics of ocean extremes such as MHWs (Wang et al., 2023; Xu et al., 2021, 2022). However, there are some caveats. Most importantly, LIMs generate long-term Gaussian statistics that are unable to capture the asymmetry between El Niño and La Niña phases (see Figure 1). Specifically, an El Niño event with certain features holds an equal probability of occurrence to a La Niña event with the same features. Thus, our LIM cannot capture observed ENSO asymmetries, with El Niño events tending to be

more intense than La Niña events, and La Niña events exhibiting greater persistence than El Niño events (Martinez-Villalobos et al., 2019; Okumura & Deser, 2010). Additionally, the LIM used in this study does not explicitly include seasonality, while still correctly capturing the phase relationships among different variables. This could pose a problem in understanding MHW impacts as stressors of marine species may exhibit seasonal influences. Coral bleaching events, for instance, are more likely to occur during summer months (Spillman & Alves, 2009). However, since here we are considering concurrent associations between MHWs and ENSO, which peaks in the boreal winter season, the explicit representation of the full seasonal cycle does not seem critical.

While a weak, positive correlation has been previously noted between SST anomalies around Hawaii and ENSO (McKenzie et al., 2019), there is little known about this relationship. By considering the difference in MHW intensity between CP and EP El Niños (Figure 2), we note that the larger meridional scale in the pattern of MHW intensity differences in Figure 2 (see also Yan et al., 1992) reaches the Hawaiian Islands during CP El Niños, indicative of MHW activity in that region. During EP El Niños, a narrow band of positive SST anomalies extending eastward to 180°E is observed along the equator, with very weak (between -0.2 and 0.2 C) SST anomalies around the Hawaiian Islands (Figure 2). Our understanding of the impacts of La Niña events in this region is limited. However, we found indications of MHWs around Hawaii during EP La Niña events as the band of enhanced MHW activity in the western Pacific extends all the way to Hawaii (Figures 2 and 3).

Our regional analysis also highlighted the connection between the Indian and Pacific Oceans, with MHWs very likely to co-occur in the Indian Ocean with El Niño events (Figures 2–4). These findings are also supported by previous studies, such as Holbrook et al. (2019), who showed ENSO to be the main driver of MHWs across much of the tropical Indian Ocean. The Pacific Ocean can affect the Indian Ocean through atmospheric bridges and the oceanic Indonesian Throughflow. For example, a positive Indian Ocean Dipole (IOD) often co-occurs with El Niño via changes in the Walker circulation (Wang et al., 2019), followed by a basin-wide warming (e.g., the Indian Ocean basin mode (Basin Mode or IOBM)), which emerges during the next boreal spring and persists in boreal summer (Xie et al., 2016). In turn, a warm Indian Ocean can also produce a La Niña-like SST pattern in the Pacific Ocean via atmospheric Kelvin waves (Wang et al., 2019). These complex ENSO-IOD/IOBM connections increase the likelihood of MHW co-occurrences in the Pacific and Indian Oceans and are key factors to consider for improving MHW prediction.

Finally, while ENSO is a well-known driver of warming in the Northeast Pacific, our analysis more specifically relates the likelihood of occurrence and intensity of MHWs in that region to the presence of CP El Niño conditions in the tropical Pacific, especially the longer-lasting conditions.

Recent research indicates that the duration and strength of El Niño and La Niña events may increase due to climate change (Cai et al., 2015; Trenberth, 2020). The data generated by long LIM simulations produced several thousand ENSO events of durations longer than 13 months, which offer valuable insights into their potential impacts. Notably, our analysis indicates heightened likelihoods of more intense MHWs associated with prolonged ENSO events. Recent studies further suggest a potential increase in the frequency of prolonged La Niña events under future greenhouse-gas forcings (Geng et al., 2023). While these future scenarios remain unseen, exploring such extraordinary ENSO events provides valuable insights into their potential implications. For instance, analyzing the impact of a “triple dip” La Niña event, akin to the 2020/21/22 occurrence, on MHWs aids in understanding extreme event dynamics that may become more frequent in the future.

Due to the potential predictability offered by ENSO for MHWs (Holbrook et al., 2019, 2020), understanding MHWs under different ENSO conditions holds significant implications for marine resource management. Discerning the details of MHW behavior across various ENSO phases can enhance the forecasting potential of these extreme events, which is of vital importance for decision-making and for the design of adaptation plans.

Conflict of Interest

The authors declare no conflicts of interest relevant to this study.

Data Availability Statement

The LIM data sets are available at Zenodo (Xu, 2024).

The HadISST observational data is open source and available for download at <https://www.metoffice.gov.uk/hadobs/hadisst/data/download.html>.

Acknowledgments

This paper presents results from a research project developed during a Summer School (July 24–29, 2023, Trieste, Italy) jointly sponsored by CLIVAR and the International Center for Theoretical Physics (ICTP) in Trieste, Italy. The project was devised in the context of the “Skill Development,” Awareness and Application (SDA2) framework developed by Dr. Shikha Singh. The authors thank CLIVAR, ICTP, US CLIVAR, NOAA, and NSF for their sponsorship and support, and Drs. Singh and Sprintall for leading the organization of the school. JS has been supported by NASA Grant 80NSSC21K0556. AC was supported by the NOAA Climate Program Office MAPP program, and by NASA Physical Oceanography Program Grant 80NSSC21K0556. CM acknowledges support from Proyecto ANID Fondecyt código 3200621, and Data Observatory Foundation ANID Technology Center No. DO210001. NJH is supported by funding from the ARC Centre of Excellence for Climate Extremes (CE170100023) and Australia’s National Environmental Science Program Climate Systems Hub. CHG is supported by the CSIRO-UTAS Quantitative Marine Sciences PhD Program.

References

- Alexander, M. A., Matrosova, L., Penland, C., Scott, J. D., & Chang, P. (2008). Forecasting Pacific SSTs: Linear inverse model predictions of the PDO. *Journal of Climate*, 21(2), 385–402. <https://doi.org/10.1175/2007jcli1849.1>
- Amaya, D. J., Miller, A. J., Xie, S.-P., & Kosaka, Y. (2020). Physical drivers of the summer 2019 North Pacific marine heatwave. *Nature Communications*, 11(1), 1903. <https://doi.org/10.1038/s41467-020-15820-w>
- Ashok, K., Behera, S. K., Rao, S. A., Weng, H., & Yamagata, T. (2007). El Niño Modoki and its possible teleconnection. *Journal of Geophysical Research*, 112(C11). <https://doi.org/10.1029/2006jc003798>
- Bond, N. A., Cronin, M. F., Freeland, H., & Mantua, N. (2015). Causes and impacts of the 2014 warm anomaly in the NE Pacific. *Geophysical Research Letters*, 42(9), 3414–3420. <https://doi.org/10.1002/2015gl063306>
- Cai, W., Santoso, A., Wang, G., Yeh, S.-W., An, S.-I., Cobb, K. M., et al. (2015). ENSO and greenhouse warming. *Nature Climate Change*, 5(9), 849–859. <https://doi.org/10.1038/nclimate2743>
- Capotondi, A., Newman, M., Xu, T., & Di Lorenzo, E. (2022). An optimal precursor of Northeast Pacific marine heatwaves and central Pacific El Niño events. *Geophysical Research Letters*, 49(5), e2021GL097350. <https://doi.org/10.1029/2021gl097350>
- Capotondi, A., & Sardeshmukh, P. D. (2015). Optimal precursors of different types of ENSO events. *Geophysical Research Letters*, 42(22), 9952–9960. <https://doi.org/10.1002/2015gl066171>
- Capotondi, A., & Sardeshmukh, P. D. (2017). Is El Niño really changing? *Geophysical Research Letters*, 44(16), 8548–8556. <https://doi.org/10.1002/2017gl074515>
- Capotondi, A., Sardeshmukh, P. D., Di Lorenzo, E., Subramanian, A. C., & Miller, A. J. (2019). Predictability of US West Coast ocean temperatures is not solely due to ENSO. *Scientific Reports*, 9(1), 10993. <https://doi.org/10.1038/s41598-019-47400-4>
- Capotondi, A., Wittenberg, A. T., Kug, J.-S., Takahashi, K., & Mepshaden, M. J. (2020). ENSO diversity. In *El Niño southern oscillation in a changing climate.* (pp. 65–86).
- Capotondi, A., Wittenberg, A. T., Newman, M., Di Lorenzo, E., Yu, J.-Y., Braconnot, P., et al. (2015). Understanding ENSO diversity. *Bulletin of the American Meteorological Society*, 96, 921–938. <https://doi.org/10.1175/bams-d-13-00117.1>
- Carrasco, D., Pizarro, O., Jacques-Coper, M., & Narvaez, D. A. (2023). Main drivers of marine heat waves in the eastern South Pacific. *Frontiers in Marine Science*, 10, 1129276. <https://doi.org/10.3389/fmars.2023.1129276>
- Cheung, W. W., & Frölicher, T. L. (2020). Marine heatwaves exacerbate climate change impacts for fisheries in the northeast Pacific. *Scientific Reports*, 10(1), 6678. <https://doi.org/10.1038/s41598-020-63650-z>
- Cresswell, G. R., & Golding, T. (1980). Observations of a south-flowing current in the southeastern Indian Ocean. *Deep-Sea Research, Part A: Oceanographic Research Papers*, 27(6), 449–466. [https://doi.org/10.1016/0198-0149\(80\)90055-2](https://doi.org/10.1016/0198-0149(80)90055-2)
- Di Lorenzo, E., & Mantua, N. (2016). Multi-year persistence of the 2014/15 North Pacific marine heatwave. *Nature Climate Change*, 6(11), 1042–1047. <https://doi.org/10.1038/nclimate3082>
- Feng, M., McPhaden, M. J., Xie, S.-P., & Hafner, J. (2013). La Niña forces unprecedented Leeuwin Current warming in 2011. *Scientific Reports*, 3(1), 1277. <https://doi.org/10.1038/srep01277>
- Gen, L., Bao-Hua, R., Cheng-Yun, Y., & Jian-Qiu, Z. (2010). Traditional El Niño and El Niño Modoki revisited: Is El Niño Modoki linearly independent of traditional El Niño? *Atmospheric and Oceanic Science Letters*, 3(2), 70–74. <https://doi.org/10.1080/16742834.2010.11446845>
- Geng, T., Jia, F., Cai, W., Wu, L., Gan, B., Jing, Z., et al. (2023). Increased occurrences of consecutive La Niña events under global warming. *Nature*, 619(7971), 774–781. <https://doi.org/10.1038/s41586-023-06236-9>
- Hobday, A. J., Alexander, L. V., Perkins, S. E., Smale, D. A., Straub, S. C., Oliver, E. C. J., et al. (2016). A hierarchical approach to defining marine heatwaves. *Progress in Oceanography*, 141, 227–238. <https://doi.org/10.1016/j.pocean.2015.12.014>
- Holbrook, N. J., Scannell, H. A., Sen Gupta, A., Benthuyesen, J. A., Feng, M., Oliver, E. C. J., et al. (2019). A global assessment of marine heatwaves and their drivers. *Nature Communications*, 10(1), 2624. <https://doi.org/10.1038/s41467-019-10206-z>
- Holbrook, N. J., Sen Gupta, A., Oliver, E. C. J., Hobday, A. J., Benthuyesen, J. A., Scannell, H. A., et al. (2020). Keeping pace with marine heatwaves. *Nature Reviews Earth & Environment*, 1(9), 482–493. <https://doi.org/10.1038/s43017-020-0068-4>
- Huang, B., Banzon, V. F., Freeman, E., Lawrimore, J., Liu, W., Peterson, T. C., et al. (2015). Extended reconstructed sea surface temperature version 4 (ERSST.v4). Part I: Upgrades and intercomparisons. *Journal of Climate*, 28(3), 911–930. <https://doi.org/10.1175/jcli-d-14-00006.1>
- Ishii, M., Shouji, A., Sugimoto, S., & Matsumoto, T. (2005). Objective analyses of sea-surface temperature and marine meteorological variables for the 20th century using ICOADS and the Kobe collection. *International Journal of Climatology: A Journal of the Royal Meteorological Society*, 25(7), 865–879. <https://doi.org/10.1002/joc.1169>
- Jacox, M. G., Alexander, M. A., Bograd, S. J., & Scott, J. D. (2020). Thermal displacement by marine heatwaves. *Nature*, 584(7819), 82–86. <https://doi.org/10.1038/s41586-020-2534-z>
- Kao, H.-Y., & Yu, J.-Y. (2009). Contrasting eastern-Pacific and central-Pacific types of ENSO. *Journal of Climate*, 22(3), 615–632. <https://doi.org/10.1175/2008jcli2309.1>
- Lenssen, N. J. L., Goddard, L., & Mason, S. (2020). Seasonal forecast skill of ENSO teleconnection maps. *Weather and Forecasting*, 35(6), 2387–2406. <https://doi.org/10.1175/waf-d-19-0235.1>
- Marshall, A., Hudson, D., Wheeler, M., Alves, O., Hendon, H., Pook, M., & Risbey, J. (2014). Intra-seasonal drivers of extreme heat over Australia in observations and POAMA-2. *Climate Dynamics*, 43(7–8), 1915–1937. <https://doi.org/10.1007/s00382-013-2016-1>
- Martínez-Villalobos, C., Newman, M., Vimont, D. J., Penland, C., & David Neelin, J. (2019). Observed El Niño-La Niña asymmetry in a linear model. *Geophysical Research Letters*, 46(16), 9909–9919. <https://doi.org/10.1029/2019gl082922>
- Mckenzie, M. M., Giambelluca, T. W., & Diaz, H. F. (2019). Temperature trends in Hawaii: A century of change, 1917–2016. *International Journal of Climatology*, 39(10), 3987–4001. <https://doi.org/10.1002/joc.6053>
- Meyers, G. (1996). Variation of Indonesian throughflow and the El Niño-southern oscillation. *Journal of Geophysical Research*, 101(C5), 12255–12263. <https://doi.org/10.1029/95jc03729>

- Neelin, J. D., Battisti, D. S., Hirst, A. C., Jin, F.-F., Wakata, Y., Yamagata, T., & Zebiak, S. E. (1998). ENSO theory. *Journal of Geophysical Research*, *103*(C7), 14261–14290. <https://doi.org/10.1029/97jc03424>
- Newman, M., Alexander, M. A., Ault, T. R., Cobb, K. M., Deser, C., Di Lorenzo, E., et al. (2016). The Pacific decadal oscillation, revisited. *Journal of Climate*, *29*(12), 4399–4427. <https://doi.org/10.1175/jcli-d-15-0508.1>
- Newman, M., & Sardeshmukh, P. D. (2017). Are we near the predictability limit of tropical Indo-Pacific sea surface temperatures? *Geophysical Research Letters*, *44*(16), 8520–8529. <https://doi.org/10.1002/2017gl074088>
- Newman, M., Shin, S.-I., & Alexander, M. A. (2011). Natural variation in ENSO flavors. *Geophysical Research Letters*, *38*(14). <https://doi.org/10.1029/2011gl047658>
- Okumura, Y. M., & Deser, C. (2010). Asymmetry in the duration of El Niño and La Niña. *Journal of Climate*, *23*(21), 5826–5843. <https://doi.org/10.1175/2010jcli3592.1>
- Pearce, A. F., & Feng, M. (2013). The rise and fall of the “marine heat wave” off Western Australia during the summer of 2010/2011. *Journal of Marine Systems*, *111*, 139–156. <https://doi.org/10.1016/j.jmarsys.2012.10.009>
- Penland, C., & Magorian, T. (1993). Prediction of Niño 3 sea surface temperatures using linear inverse modeling. *Journal of Climate*, *6*, 1067–1076. [https://doi.org/10.1175/1520-0442\(1993\)006<1067:ponss>2.0.co;2](https://doi.org/10.1175/1520-0442(1993)006<1067:ponss>2.0.co;2)
- Penland, C., & Sardeshmukh, P. D. (1995). The optimal growth of tropical sea surface temperature anomalies. *Journal of Climate*, *8*, 1999–2024. [https://doi.org/10.1175/1520-0442\(1995\)008<1999:togots>2.0.co;2](https://doi.org/10.1175/1520-0442(1995)008<1999:togots>2.0.co;2)
- Rayner, N., Parker, D. E., Horton, E., Folland, C. K., Alexander, L. V., Rowell, D., et al. (2003). Global analyses of sea surface temperature, sea ice, and night marine air temperature since the late nineteenth century. *Journal of Geophysical Research*, *108*(D14). <https://doi.org/10.1029/2002jd002670>
- Ren, X., Liu, W., Capotondi, A., Amaya, D. J., & Holbrook, N. J. (2023). The Pacific Decadal Oscillation modulated marine heatwaves in the Northeast Pacific during past decades. *Communications Earth & Environment*, *4*(1), 218. <https://doi.org/10.1038/s43247-023-00863-w>
- Sen Gupta, A., Thomsen, M., Benthuisen, J. A., Hobday, A. J., Oliver, E., Alexander, L. V., et al. (2020). Drivers and impacts of the most extreme marine heatwave events. *Scientific Reports*, *10*(1), 19359. <https://doi.org/10.1038/s41598-020-75445-3>
- Smale, D. A., Wernberg, T., Oliver, E. C. J., Thomsen, M., Harvey, B. P., Straub, S. C., et al. (2019). Marine heatwaves threaten global biodiversity and the provision of ecosystem services. *Nature Climate Change*, *9*(4), 306–312. <https://doi.org/10.1038/s41558-019-0412-1>
- Smith, K. E., Burrows, M. T., Hobday, A. J., King, N. G., Moore, P. J., Sen Gupta, A., et al. (2023). Biological impacts of marine heatwaves. *Annual Review of Marine Science*, *15*(1), 119–145. <https://doi.org/10.1146/annurev-marine-032122-121437>
- Smith, K. E., Burrows, M. T., Hobday, A. J., Sen Gupta, A., Moore, P. J., Thomsen, M., et al. (2021). Socioeconomic impacts of marine heatwaves: Global issues and opportunities. *Science*, *374*(6566), eabj3593. <https://doi.org/10.1126/science.abj3593>
- Spillman, C. M., & Alves, O. (2009). Dynamical seasonal prediction of summer sea surface temperatures in the Great Barrier Reef. *Coral Reefs*, *28*(1), 197–206. <https://doi.org/10.1007/s00338-008-0438-8>
- Student. (1908). The probable error of a mean. *Biometrika*, *6*, 1–25. <https://doi.org/10.2307/2331554>
- Sullivan, A., Luo, J.-J., Hirst, A. C., Bi, D., Cai, W., & He, J. (2016). Robust contribution of decadal anomalies to the frequency of central-Pacific El Niño. *Scientific Reports*, *6*(1), 38540. <https://doi.org/10.1038/srep38540>
- Takahashi, K., Montecinos, A., Goubanova, K., & Dewitte, B. (2011). ENSO regimes: Reinterpreting the canonical and Modoki El Niño. *Geophysical Research Letters*, *38*(10). <https://doi.org/10.1029/2011gl047364>
- Timmermann, A., An, S.-I., Kug, J.-S., Jin, F.-F., Cai, W., Capotondi, A., et al. (2018). El Niño–southern oscillation complexity. *Nature*, *559*(7715), 535–545. <https://doi.org/10.1038/s41586-018-0252-6>
- Trenberth, K. E. (2020). Understanding climate change through Earth’s energy flows. *Journal of the Royal Society of New Zealand*, *50*(2), 331–347. <https://doi.org/10.1080/03036758.2020.1741404>
- Vimont, D. J., Alexander, M. A., & Newman, M. (2014). Optimal growth of central and east Pacific ENSO events. *Geophysical Research Letters*, *41*(11), 4027–4034. <https://doi.org/10.1002/2014gl059997>
- Wallace, J. M., Rasmusson, E. M., Mitchell, T. P., Kousky, V. E., Sarachik, E. S., & Von Storch, H. (1998). On the structure and evolution of ENSO-related climate variability in the tropical Pacific: Lessons from TOGA. *Journal of Geophysical Research*, *103*(C7), 14241–14259. <https://doi.org/10.1029/97jc02905>
- Wang, H., Kumar, A., Murtugudde, R., Narapusetty, B., & Seip, K. L. (2019). Covariations between the Indian Ocean Dipole and ENSO: A modeling study. *Climate Dynamics*, *53*(9–10), 5743–5761. <https://doi.org/10.1007/s00382-019-04895-x>
- Wang, Y., Holbrook, N. J., & Kajtar, J. B. (2023). Predictability of marine heatwaves off Western Australia using a linear inverse model. *Journal of Climate*, *36*(18), 1–40. <https://doi.org/10.1175/jcli-d-22-0692.1>
- Wyatt, A. M., Resplandy, L., & Marchetti, A. (2022). Ecosystem impacts of marine heat waves in the Northeast Pacific. *Biogeosciences*, *19*(24), 5689–5705. <https://doi.org/10.5194/bg-19-5689-2022>
- Xie, S.-P., Kosaka, Y., Du, Y., Hu, K., Chowdary, J. S., & Huang, G. (2016). Indo-western Pacific Ocean capacitor and coherent climate anomalies in post-ENSO summer: A review. *Advances in Atmospheric Sciences*, *33*(4), 411–432. <https://doi.org/10.1007/s00376-015-5192-6>
- Xu, T. (2024). Long simulation of global Sea Surface temperature using linear inverse model [Dataset]. *Zenodo*. <https://doi.org/10.5281/zenodo.11397241>
- Xu, T., Newman, M., Capotondi, A., & Di Lorenzo, E. (2021). The continuum of Northeast Pacific marine heatwaves and their relationship to the tropical Pacific. *Geophysical Research Letters*, *48*(2), 2020GL090661. <https://doi.org/10.1029/2020gl090661>
- Xu, T., Newman, M., Capotondi, A., Stevenson, S., Di Lorenzo, E., & Alexander, M. A. (2022). An increase in marine heatwaves without significant changes in surface ocean temperature variability. *Nature Communications*, *13*(1), 7396. <https://doi.org/10.1038/s41467-022-34934-x>
- Yan, X.-H., Ho, C.-R., Zheng, Q., & Klemas, V. (1992). Temperature and size variabilities of the western Pacific warm pool. *Science*, *258*(5088), 1643–1645. <https://doi.org/10.1126/science.258.5088.1643>
- Zhang, N., Feng, M., Hendon, H. H., Hobday, A. J., & Zinke, J. (2017). Opposite polarities of ENSO drive distinct patterns of coral bleaching potentials in the southeast Indian Ocean. *Scientific Reports*, *7*(1), 2443. <https://doi.org/10.1038/s41598-017-02688-y>